Appl. Phys. B 80, 101–107 (2005)
DOI: 10.1007/s00340-004-1672-6

Applied Physics B
Lasers and Optics

A.S. MOORE✉
K.J. MENDHAM
D.R. SYMES
J.S. ROBINSON
E. SPRINGATE
M.B. MASON
R.A. SMITH
J.W.G. TISCH
J.P. MARANGOS

Control parameters for ion heating and X-ray emission from laser induced cluster explosion

Blackett Laboratory, Imperial College London, Prince Consort Road, London, SW7 2BW, United Kingdom

Received: 16 July 2004/Revised version: 10 September 2004
Published online: 26 October 2004 •

ABSTRACT The highest energies of the ions obtained from the explosion of an atomic cluster in an intense femtosecond laser field can vary greatly depending on the cluster size, atomic species and the peak intensity, duration and shape of the laser pulse. By careful choice of these parameters the ion energies, electron energies or X-ray emission can be optimised. A relationship is described that allows for rapid determination of the optimum experimental parameters. We present experimental data of keV X-ray emission from Argon clusters, which investigate intensity and pulse duration effects. In addition we present the first results from closed-loop optimal control, pulse-shaping experiments that optimise X-ray emission and show a significant enhancement in the X-ray yield.

PACS 36.40.Gk; 52.50.Jm

1 Introduction

When subject to an intense femtosecond laser field, atomic clusters can generate keV electrons, maximum ion energies up to ∼ MeV, and strong X-ray emission [1–3] owing to the microscopic, solid density of the cluster. Such an interaction is consequently very efficient at absorbing the laser energy, greater than 95% absorption has been measured [4]. In accord with such exceptional properties, substantial experimental and numerical modelling now exists on the subject, see reviews [5, 6]. Laser energy can be channelled into either ion or electron energies, which will affect the macroscopic X-ray emission. The particle energies and X-ray emission critically depend on certain parameters such as the mean cluster size and species, and the intensity and shape of the irradiating laser pulse [7–10]. A number of experiments have been conducted investigating the parameter scaling of the laser-cluster interaction, which have shown that for a given laser pulse, defined by its peak intensity and pulse duration, there is a particular cluster size that absorbs the most laser energy and produces ions with the highest energies.

This report begins by discussing an empirical formula that can be used to estimate the size of cluster that gives rise to the highest energy ions when irradiated by a high-intensity, femtosecond laser pulse for a given laser intensity, pulse duration and cluster species, which we term the optimum cluster size. Knowing the optimum cluster size for particular experimental parameters is important for achieving the maximum laser energy absorption and maximising the ion kinetic energy [1].

Springate et al. conducted an experiment measuring the energies of the ions emitted from an exploding Xe cluster as a function of cluster size [7]. The results show an increase in ion energy by a factor of ∼6 at the optimum cluster size compared to the smallest cluster studied. Zweiback et al. have measured the absorption of the laser energy and the scatter from variously sized Xe clusters as a function of laser pulse duration [8]. Again, a peak was observed in the data signifying an optimum duration laser pulse, which varied with cluster size. The extreme-ultraviolet (EUV) radiation emitted from expanding Xe clusters was studied by Schnürer et al. [9] for two different laser pulse durations. A peak in the EUV emission was measured for each pulse duration as the cluster size was varied. More recently, Caillaud et al. looked at the intensity of the He_α emission line (at 3.14 keV) from Ar clusters as a function of laser pulse duration for three different cluster sizes [10]. Optimum pulse durations were recorded for each cluster size that increases with the cluster radius for the range of sizes investigated.

The ability to predict the optimum parameters for an experiment can be used in conjunction with feedback-controlled laser-pulse shapers now incorporated in many laser systems. Feedback control can optimise the cluster explosion in a number of ways, reliant on the parameter for which optimisation is sought. A closed-loop experiment can be run to optimise the X-ray emission, electron energy or ion energy to best determine what shape of laser pulse will maximise the explosion products. This provides an objective insight to help explain the underlying interaction physics of the laser-cluster interaction. When maximising the production of high-energy photon, electron and ion sources, this method could be of great value in enhancing the efficiency of production. Furthermore, when running such routines, an empirical formula is of assistance in ensuring that the routine does not find a local maximum, and that the optimisation routines are improving on what can already be achieved by careful choice of the laser pulse and cluster parameters used for the experiment in question.

✉ Fax: +44-20-7594-7714, E-mail: alastair.moore@physics.org

2 Numerical modelling: scaling of maximum ion energy with laser-cluster parameters

The high degree of interest in using clusters as an energetic ion and XUV source, has motivated a number of investigations of how to optimise ion production and X-ray emission both theoretically and by experiment. Previous theoretical investigations have produced very useful expressions, which match experimental data well, and estimate the maximum ion energy produced from clusters that explode in the coulomb regime, typically valid for small, low-Z clusters [11]. These also estimate the minimum laser intensity necessary to expel all the electrons from the cluster, creating conditions for a coulomb explosion. Unfortunately these are not applicable for large, high-Z clusters or at moderately high intensities, where hydrodynamic forces are responsible for the explosion kinematics. As such they do not enable the prediction of the best cluster conditions for a specific laser pulse duration or intensity to maximise ion or X-ray production from clusters of the type we investigate.

We investigate the cluster explosion according to the well-known nanoplasma model of the interaction with the aim of relating cluster and laser conditions to identify a cluster size that maximises the energy coupling to ions in the cluster [12]. Although other hydrodynamic and PIC code models exist [13, 14] that eliminate some of the assumptions inherent in the nanoplasma model, in the regime studied here, where for the experimental case the cluster size is less than the laser skin depth (≈ 100 Å) and greater than the Debye length inside the cluster (≈ 10 Å), it is appropriate to make use of a uniform density model, since the electric field will be uniform throughout the cluster. The cause of the strong dependence on cluster size and species, laser intensity and pulse duration is through the Mie-like resonance that occurs during the cluster heating. It is at this resonance that the majority of the cluster heating occurs through collisional absorption and so the timing of the resonance during the laser pulse makes a large difference to the ion energies that can be obtained from the exploding cluster. The timing depends upon the parameters of the cluster and of the laser pulse. Large, high-Z clusters expand more slowly than small, low-Z clusters, taking longer to reach the resonance position. To produce the highest energy ions the optimum cluster size for a long laser pulse is larger than for that for a short laser pulse. The laser intensity also affects the timing of the resonance, since a higher intensity laser pulse initiates ionisation and the cluster expansion earlier in the pulse and causes a more rapid expansion of the cluster. Therefore a short, high-intensity laser pulse has an optimum cluster size that is smaller than that of a long, low-intensity laser pulse.

A series of simulations for Ar, Kr and Xe clusters has been conducted using the nanoplasma model [12] to determine the size of cluster that gives rise to the highest energy ions as a function of cluster species, pulse duration and peak laser intensity for a Gaussian laser pulse of centre wavelength 800 nm. This will eliminate the computationally demanding task of running the model for every experiment, enabling a rapid estimation of the optimum laser-cluster parameters. We obtain from these simulations an empirical formula that fits the experimental data well. Two of the three parameters were fixed in turn and the third was varied.

The empirical formula we find is:

$$N_{\mathrm{c}}(\mathrm{opt}) = \left(\frac{4}{3}\pi\varrho R_{\mathrm{c}}(\mathrm{opt})\right)^3 \approx 1.8\times10^{-13}\, Z^{-1} I^{0.75}\,(\mathrm{W\,cm^{-2}})\tau^3\,(\mathrm{fs}) \quad (1)$$

where $N_{\mathrm{c}}(\mathrm{opt})$ is the optimum number of atoms per cluster, ϱ is the density inside the cluster, $R_{\mathrm{c}}(\mathrm{opt})$ is the optimum cluster radius, Z is the atomic number of the cluster species, $\tau < 400$ fs is the FWHM (Gaussian) laser pulse duration and $I < 1\times10^{17}\,\mathrm{W\,cm^{-2}}$ is the laser peak intensity. These upper limits of τ and I correspond to an optimum cluster radius of ≈ 125 Å for Xe clusters. For pulse durations longer than 400 fs, simulations show the optimum cluster size increasing less rapidly with pulse duration. Due to the lack of experimental results showing the optimum cluster size for low-Z clusters such as hydrogen and deuterium the validity of the above formula has not been verified for these species. Indeed, due to the more coulombic explosion that occurs in low-Z clusters it is expected that the formula will not be valid in this regime.

The cubic dependence on laser pulse duration can be understood in terms of the time taken for the cluster to reach its resonance, which can be shown to be [8]:

$$\tau_{\mathrm{R}} = \frac{r_0}{v}\left[\left(\frac{n_0}{3n_{\mathrm{crit}}}\right)^{\frac{1}{3}} - 1\right] \quad (2)$$

where r_0 is the initial cluster radius, v is the expansion velocity, n_0 is the initial density in the cluster and n_{crit} is the critical density. We have been unable to provide a simple explanation for the other scalings owing to the complexity of the interplay involved in cluster ionisation and heating. This complexity is indeed the motivation for our empirical formula. Previous investigations of high-energy ion production from clusters by Zhu et al. found that the mean ion kinetic energy from Ar ions was maximised for 35 Å radius cluster irradiated at $1.5\times10^{16}\,\mathrm{W\,cm^{-2}}$, within a factor of two of the radius predicted by our empirical formula [15].

2.1 *Comparison with experimental data*

Figure 1 shows a comparison of the optimum cluster size as determined using the nanoplasma computer model (scatter graphs) and (1) (line graphs). Results are shown for three cluster species, Ar (squares and solid line), Kr (triangles and dashed line) and Xe (circles and dotted line). Figure 1a shows the optimum cluster size as a function of peak laser intensity for a laser pulse of duration 80 fs. Figure 1b shows the optimum cluster size as a function of laser pulse duration at a fixed peak intensity of $1\times10^{16}\,\mathrm{W\,cm^{-2}}$. In both cases, the results agree with the full nanoplasma model within a maximum error of 18% in the number of atoms per cluster. This corresponds to an uncertainty of 6% in the optimum cluster radius. Given that the supersonic nozzles typically used for cluster production do not produce a single cluster size but a lognormal distribution of sizes [16] this uncertainty will not be significant experimentally.

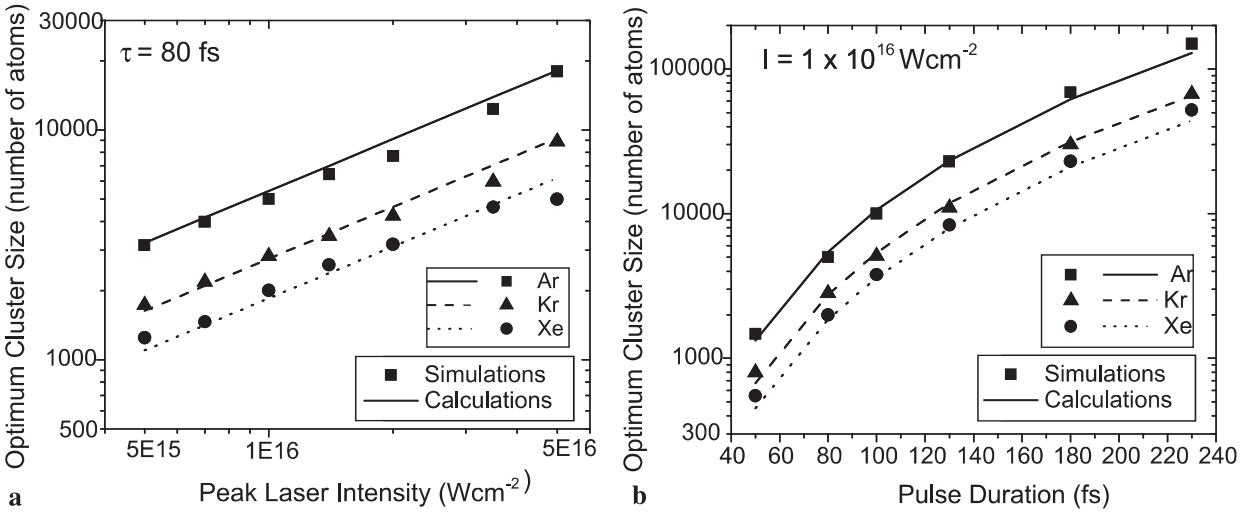

FIGURE 1 Comparison of the optimum cluster size as given by simulations conducted with the nanoplasma model and calculation using (1). Results are shown for three different cluster species as (**a**) a function of laser intensity at a fixed pulse duration of 80 fs and (**b**) as a function of pulse duration at a fixed peak laser intensity of 1×10^{16} W cm^{-2}

Figure 2 shows four cases where the optimum cluster size predicted by (1) (black crosses) is compared to experimental results (other symbols) for different peak laser intensities and pulse durations. The triangle corresponds to the work of Springate et al. [6]. Experimental results showed an optimum cluster size of $10\,000 \pm 5000$ Xe atoms, while (1) predicts an optimum of 17 800 atoms per cluster. A jet of clusters with mean size 10 000 atoms would contain clusters of 17 800 atoms within the log-normal distribution [17]. The square corresponds to previous experimental work by the author [17], again (1) predicts an optimum cluster size in good agreement with experimental results. The blue line shows the range within which the optimum cluster size occurs in experimental work by Ditmire et al. [12]. Ditmire measured the Ar^{7+} signal as a function of gas backing pressure from clusters irradiated with laser pulses of duration 125 fs and peak intensity 2×10^{16} W cm^{-2}. An optimum in signal is seen at a backing pressure of ≈ 400 psi, corresponding to a cluster size in the range 8000–28 000 atoms. This implies that the maximum absorption of the laser energy also occurs at this cluster size since further results published within the same report show the Ar^{7+} and Ar^{8+} signals are both optimised at the same time. (1) predicts an optimum cluster size of $\approx 20\,000$ Ar atoms, in excellent agreement with the experimental data. The other set of data shown in Fig. 2a (green circle) is previously unpublished experimental data. The energies of the ions obtained from Xe clusters irradiated with 90 fs laser pulses of peak intensity 2×10^{16} W cm^{-2} were measured as a function of cluster size by changing the jet backing pressure. A peak in both the maximum and the mean ion energies was measured at a cluster size of ~ 7000 atoms, in close agreement with the prediction of (1). Figure 3 shows the measured mean ion energies and a polynomial fit to them. The vertical line shows the optimum cluster size predicted using (1).

The experimental work of Caillaud et al. [10] and Zweiback et al. [8] measure X-ray emission from Ar clusters as a function of laser pulse duration while keeping the laser energy constant. Both data sets find optimum pulse durations

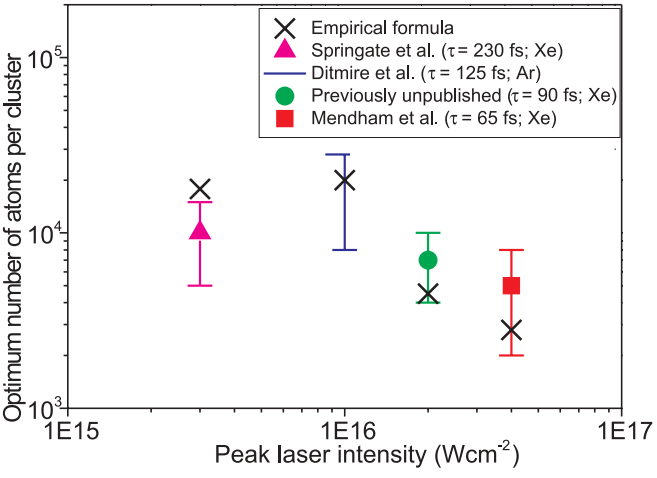

FIGURE 2 A comparison of the experimental work of Springate et al. [6] (*triangle*), Mendham et al. [17] (*square*), Ditmire et al. [12] (*blue line*) and previously unpublished experimental data shown (*circle*) to the predictions of (1) (*black crosses*)

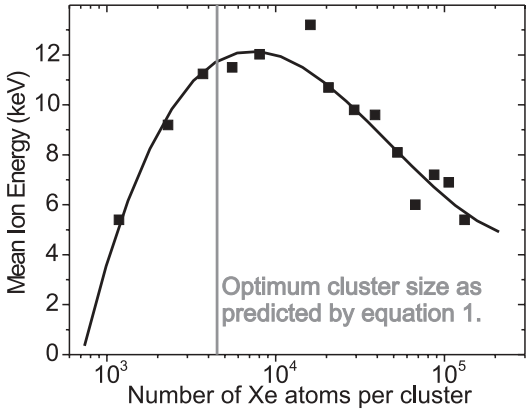

FIGURE 3 Experimental data showing the mean ion energy as a function of cluster size for a Xe cluster irradiated with a laser pulse of duration 90 fs and peak intensity 2×10^{16} W cm^{-2}. The vertical line represents the cluster size that (1) predicts as the optimum for these laser parameters

that differ from those predicted by (1). Caillaud et al. determine a peak in the He_α emission line intensity at a pulse duration of ~ 150 fs when irradiating a 180 Å radius cluster with a laser pulse of peak intensity $\sim 2 \times 10^{16}$ W cm^{-2}. Zweiback et al. measure the X-ray emission from a smaller cluster (110 Å) with a slightly higher intensity laser pulse ($\approx 3.5 \times 10^{16}$ W cm^{-2}). This should result in a shorter optimum pulse duration being measured than for the 180 Å clusters; instead an optimum of 275 fs is measured, making the two sets of data inconsistent. (1) predicts that a 110 Å cluster irradiated with the laser system of Zweiback et al. will have an optimum pulse duration of 150 fs, and the 180 Å cluster irradiated with the laser system used by Caillaud et al. will have an optimum at 425 fs.

3 Experiments for close-loop control optimisation of X-ray emission

3.1 *Introduction*

One clear distinction between these results and the empirical model is that the empirical formula aims to predict conditions for maximising ion energies, while these last two results are concerned with maximising X-ray emission of a single emission line. There is no clear reason why optimising the production of maximum energy ions would correspond to an optimum in X-ray emission. The underlying physics is abstruse because of the complex exchange of energy between ions and electrons, which also leads to the creation of high charge states. Previously optimal-control experiments have studied the enhancement in the yield of high charge states from the laser interaction with large Xe clusters by manipulation of laser pulse shape [18]. However, in an effort to understand the relationship between cluster heating and X-ray production, we have performed X-ray optimisation experiments in Ar clusters.

3.2 *Experimental setup*

We explore the effect of pulse duration on cluster heating in different sizes of argon clusters produced with a pulsed valve with nozzle diameter of 0.6 mm, and gas jet half angle of 45 degrees. The pulsed valve was backed with a pressure of ≈ 200 psi, producing clusters with a mean radius of 37 Å. The empirical formula can be manipulated to yield an optimum pulse duration for a given cluster size. (1) predicts an optimum pulse duration, corresponding to the clusters we produce, of 120 fs. The effect of pulse duration and temporal shape on the production of X-rays was studied in two ways: changing the compressor grating separation in the laser system, and using a phase-only pulse shaper. The latter consisting of a spatial light modulator (SLM) implemented to change the phase of different frequency components in the laser pulse. X-ray emission was detected using an AXUV100 PIN diode transmissively filtered by 2 μm of aluminium to measure X-rays of energy > 500 eV. The quantum efficiency of the device is shown in the inset to Fig. 4.

The laser used in these experiments is a Ti:sapphire laser producing pulses with a minimum pulse duration of 85 fs and delivering a maximum energy on target of 5 mJ. Variation in the compressor grating separation enabled the pulse duration

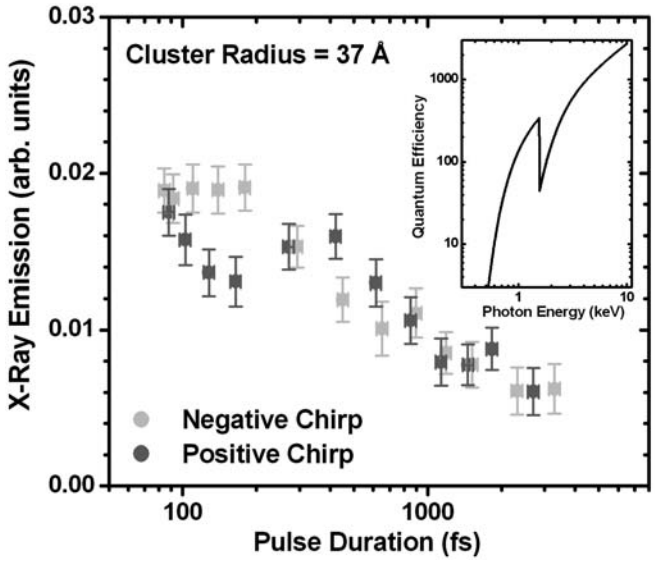

FIGURE 4 Experimental data showing the change in X-ray signal (> 500 eV) from Ar clusters with radius of 3.7 nm, when irradiated with a pulse with duration from 90 to 3000 fs. The *inset* shows the quantum efficiency of the AXUV100 PIN Diodes in the range 500 to 10 000 eV, when filtered by a 2 μm Aluminium filter

to be varied in a range from 85–3000 fs, and an $f/8$ focusing system produced peak intensities of $\approx 2 \times 10^{16}$ W cm^{-2}. Diagnosis of the laser pulse shape and pulse duration was carried out through frequency resolved optical gating (FROG) and using a single-shot autocorrelator with a 200 μm thick KDP crystal. Longer pulse durations (> 500 fs) were measured by comparing the autocorrelation measurements with the second harmonic energy from a further second harmonic crystal. The FROG was designed around the polarisation gating technique so there are no time-symmetry ambiguities [19], and images enabled the detection pulses in a 1200 fs time window.

The SLM was situated after the regenerative amplifier in the laser system (pulse energy and duration are 2 mJ and 300 ps respectively) before the power amplifier and grating compressor. The SLM is a Jenoptik (SLM-S 640/12) device with 640 pixels [20]. Each pixel has a 12-bit voltage resolution that allows the phase of each frequency component to be changed by up to 8π. Situated in the Fourier plane of an all-reflective, grating null stretcher, the SLM was aligned to the central wavelength of the laser 796.5 nm, with the 20 nm of bandwidth (FWHM) dispersed across the centre half of the pixels. Application of $\pi/2$ voltage steps to the SLM modulated the spectral phase, leading to a simple way to simultaneously calibrate the time and frequency domain of the FROG image [21]. A computer controlled the voltages applied to the SLM. This was linked to a genetic algorithm (GA) to allow feedback from the experiment to control the pulse shaper. In brief, the GA began with a population of 50 randomly generated members, each member corresponding to a set of voltages applied to the SLM. The 640 pixels were controlled in blocks of 16, so that there were effectively 40 pixel groups available, to limit the parameter space and run-time of the GA. The voltage applied to the pixel groups was limited to a range of 2π. Each member was tested in sequence; the fitness of each member was calculated by taking the ratio of the laser energy and X-ray emission averaged over 30 shots.

Five members were carried directly from one generation to the next, while the remaining 45 were generated through the interbreeding of other members according to their fitness, with a 4% mutation rate to enable the coverage of a substantial fraction of the parameter space.

4 Experimental results & discussion

4.1 *Pulse duration dependance*

The X-ray emission was first measured as a function of pulse duration for both positively and negatively chirped pulses, by varying the compressor grating separation. The energy was kept constant throughout and all data points were averaged over 60 shots, and energy binned between 3 and 3.3 mJ representing a peak intensity of $\approx 1 \times 10^{16}\,\mathrm{W\,cm^{-2}}$. Results of the compressor-grating scan are shown in Fig. 4. For negatively chirped pulses of duration between 85 ± 20 and 180 ± 20 fs, X-ray emission is maximised; for longer pulse durations the signal drops to less than 40% of this maximum at 3000 fs. Positively chirped pulses produce a different response; we find maximum X-ray emission occurs for pulses of 85 fs, but a second peak is observed at about 420 ± 30 fs. The data for negatively chirped pulses in part agrees with the pulse duration of 120 fs, predicted by (1). However, the positively chirped pulses seem to contradict this producing the maximum X-ray emission for the shortest pulse duration.

4.2 *Pulse shaping*

The results of the optimisation of X-ray emission using the pulse shaper are presented in Fig. 5. Before the algorithm was run the separation of the compressor gratings was increased to produce a negatively chirped pulse of duration 680 ± 20 fs, to observe the effect of the pulse shaper from a less optimum situation. A FROG image of this pulse is shown in 5a. Careful averaging was used to ensure the algorithm was operating in a regime where noise due to laser energy fluctuations over a long time-scale (≈ 1 hr) would not skew the results. The ratio of the PIN diode voltage and laser energy (or fitness) was fed into the algorithm and weighted the breeding. A 125% increase in the X-ray yield resulted from the evolution of the GA for ten generations, shown in c. The effect of the optimisation on the pulse shape can be seen in b and d. Both the FROG image after optimisation b and autocorrelation results show the pulse duration was shortened to a broad envelope of 360 ± 30 fs. The FROG image b and autocorrelation, upper part of d, show the introduction of sig-

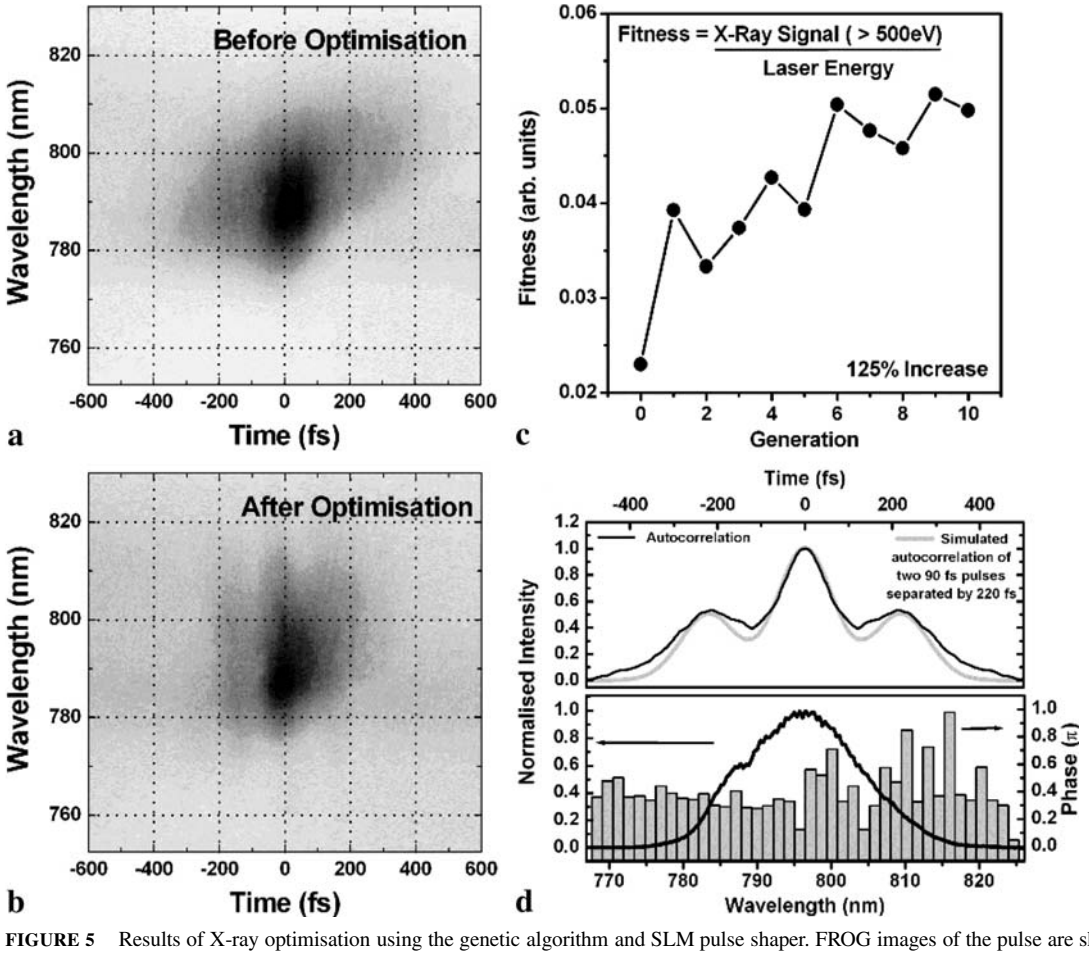

FIGURE 5 Results of X-ray optimisation using the genetic algorithm and SLM pulse shaper. FROG images of the pulse are shown before (**a**) and after (**b**) optimisation (signal dip at 790 nm, -100 fs is a damaged pixel area). The fitness function is shown during the evolution in (**c**), and the laser spectrum and phase profile that produced the optimum X-ray yield is shown in the *lower part* of (**d**). The autocorrelation result is shown in the *upper part* of (**d**) with a simulated autocorrelation trace of two 90 fs pulses separated by 220 fs

nificant structure to the pulse. The spectrum of the laser and phase elements applied by the SLM that produced the best X-ray emission as found by the GA are also shown in the lower half of d.

4.3 *Discussion*

There is clear evidence of a pulse duration dependence of the cluster explosion from the data in Fig. 4, and this in part agrees with the optimum pulse duration predicted by the empirical formula. The positively chirped data is more difficult to interpret. For the > 500 eV X-ray emission we observe, the charge state distribution is possibly one of the most closely related functions to the X-ray emission, as this will undoubtedly determine the available atomic transitions through which radiation can be produced. In a recent paper [22] particle emissions are measured as a function of pulse duration and chirp in Xe clusters. An optimum pulse duration of 500 fs is found for their experimental conditions, which is outside the range over which the empirical formula is expected to be valid, and for both ion and electron particle distributions, negatively chirped pulses are observed to maximise particle energies. However, no such clear dependence is observed in the charge state distributions, indicating that this may not be the optimal situation for producing X-ray emission. A simple analysis using the cluster-heating rate [12] indicated that due to shorter wavelengths being present in the first half of a negatively chirped pulse, that these may be better suited to heating clusters. While this is expected to be a small effect, this is in partial agreement with the chirp dependence data presented here, where a greater emission is measured for negatively chirped pulses, of short duration.

The results of the GA controlled optimisation confirm that a shorter pulse is required to maximise the X-ray emission. However, the presence of structure in the pulse will have a significant effect on the time when the cluster passes through the $3n_{\mathrm{crit}}$ resonance, as described by (2). While the GA optimisation does not find the 120 fs pulse conjectured from the empirical formula, the investigation that led to (1) is not generalised to include shaped pulses. Pre-pulse at the level seen in the autocorrelation (upper part of d) will clearly start the cluster expansion earlier than otherwise leading to an outcome different to that expected by (1). Investigations by Auguste et al., of pre-pulse effects on a timescale slightly less than the plasma expansion (~ 1–10 ps) predicted that the charge state was determined by the prepulse flux density while the temperature of electrons that interact with the charge state distribution is controlled by the higher intensity femtosecond pulse [23]. An accurate reconstruction of the autocorrelation found in our pulse shaping experiment can be made using two equal intensity pulses, of duration ≈ 90 fs separated by ≈ 220 fs. The pulses are separated by a time that is much less than the plasma expansion investigated by Auguste et al., indicating that a different mechanism to that which they describe is responsible for the high X-ray yield. The pulse shape was then used in conjunction with the nanoplasma model to aid the interpretation of the results.

Initially, during a cluster expansion the electron density rises quickly through the $3n_{\mathrm{crit}}$ resonance, but as the cluster expands the electron density drops so at a later time the resonance is passed again. Original results from the nanoplasma model [12] show that the second transition through the resonance is responsible for the high keV electron temperatures observed in cluster explosions. A comparison of electron and ion energies produced by the two-pulse structure found after optimisation and the long single pulse prior to optimisation was made using the nanoplasma model. Results show that significantly more of the energy is deposited into electrons by the pulse-shape found by the GA optimisation. The average energy per electron increases seven-fold from 10 eV, in the 680 fs, single pulse prior to optimisation, to ≈ 74 eV. At the same time the maximum ion energy only changes by a factor of 1.5 to ≈ 26 keV. The pulse structure is also significant since nanoplasma modelling indicates that a single short 90 fs pulse does not heat the electrons as efficiently as the double pulse we find as a result of the optimisation. Approximately a third of these electrons free-stream out of the cluster, while the remainder of the electrons collisionally heat the remaining ions producing the high charge states. Radiation due to electron recombination will occur on a longer ns-timescale when the high charge state (Ar^{9+}), argon plasma, releases radiation in the 500 eV region, within the detection range we measure with the PIN diode.

In the double pulse structure, the two pulses are separated by approximately 220 fs, which corresponds well with the timescale for the electron density to drop back through the resonance. Indeed the time-evolution of the laser electric field penetration inside the cluster shows significant evidence for this. The first pulse initiates the explosion, causing the electron density to rise and preventing the electric field penetrating into the cluster. For this first pulse alone, the second $3n_{\mathrm{crit}}$ resonance occurs a time 130 fs after the peak of the first pulse, on the leading edge of the second pulse. As a result, the arrival of the second pulse is well-timed to enable almost the entire electric field of the second laser pulse to penetrate into the cluster, and contribute to electron heating. We therefore conclude that rather than interacting with a "clumpy" plasma as suggested by Auguste et al. the second pulse arriving on a shorter ≈ 100 fs timescale interacts with clusters, just after the $3n_{\mathrm{crit}}$ resonance heating occurs and electron shielding stops. This provides an additional boost to the heating of all the explosion products, but a greater proportional increase to the electrons which are now all effected by the laser field, increasing the average electron energy, more efficiently driving the bremsstrahlung radiation process and creating higher charge states.

Two pulse laser cluster interactions have been investigated previously [24], the results of which indicate that higher ion energies can also be achieved through double pulse irradiation of clusters. Very recent work by Zamith et al. investigated charge state production by shaping the laser pulse through an iterative closed-loop evolution, and found evidence for the existence of a specific time when the laser field can be most efficiently coupled into the cluster plasma, in strong agreement with the double pulse result we find [25]. Therefore, finding a double pulse as a result of a freely evolved X-ray optimisation is strong confirmation of these previous studies, applied to the topic of X-ray emission rather than ion production.

5 Conclusion

We have presented an empirical formula, based on the well-established nanoplasma computer model, that predicts the optimum cluster size for maximising the energy of ions produced in high-Z, laser-cluster interactions for a given cluster species, laser pulse duration and laser peak intensity. We have shown that it is in good agreement with the relatively small number of experimental data points available for comparison, and other theoretical investigations.

Experimental data measuring X-ray emission as a function of pulse duration indicate that an optimum pulse duration does exist for a single Gaussian laser pulse and a specific cluster size, but is only in partial agreement with the empirical formula; this highlights the fact that different mechanisms could be important when X-ray emission is optimised as opposed to particle energies, due to the complicated plasma heating dynamics. Closed-loop control experiments, to optimise the X-ray emission, indicate that, in addition to the existence of an optimum pulse duration for a single pulse laser-cluster interaction, a double-pulse, on the timescale of the resonance ~ 100 fs, can still more efficiently heat clusters to maximise X-ray emission. This succeeds by initiating the cluster explosion with the first pulse and then heating with the second pulse only once electron screening ceases, which is in good agreement with the very recent work of [25].

ACKNOWLEDGEMENTS This work was funded by the EPSRC. The authors would like to acknowledge the assistance of N. Syassen and A. Noëls and excellent technical support from B. Ratnasekara, A. Gregory and P. Ruthven.

REFERENCES

1 T. Ditmire, J.W.G. Tisch, E. Springate, J P. Marangos, M.H.R. Hutchinson: Nature **386**, 54 (1997)
2 Y.L. Shao, T. Ditmire, J.W.G. Tisch, E. Springate, J.P. Marangos, M.H.R. Hutchinson: Phys. Rev. Lett. **77**, 3343 (1996)
3 T. Ditmire, T. Donnelly, R.W. Falcone, M.D. Perry: Phys. Rev Lett. **75**, 3122 (1995)
4 T. Ditmire, R.A. Smith, J.W.G. Tisch, M.H.R. Hutchinson: Phys. Rev. Lett. **78**, 3121 (1997)
5 J.W.G. Tisch, N. Hay, K.J. Mendham, E. Springate, D.R. Symes, A.J. Comley, M.B. Mason, E.T. Gumbrell, T. Ditmire, R.A. Smith, J.P. Marangos, M.H.R. Hutchinson: Nucl. Instrum. Methods Phys. Res. B **205** 310 (2003)
6 V.P. Krainov, M.B. Smirnov: Phys. Rep. **370**, 237 (2002)
7 E. Springate, N. Hay, J.W.G. Tisch, M.B. Mason, T. Ditmire, M.H.R. Hutchinson, J P. Marangos: Phys. Rev. A **61**, 063 201 (2000)
8 J. Zweiback, T. Ditmire, M.D. Perry: Phys. Rev. A **59**, R3166 (1999)
9 M. Schnürer, S. Ter-Avetisyan, H. Stiel, U. Vogt, W. Radloff, M. Kalashnikov, W. Sandner, P.V. Nickles: Eur. Phys. J. D **14**, 331 (2001)
10 T. Caillaud, F. Blasco, F. Dorchies, Y. Glinec, C. Stenz, J. Stevefelt: Nucl. Instr. Methods Phys. Res., Sect. B **205**, 329 (2003)
11 S. Sakabe, S. Shimizu, M. Hashida, T. Tsuyukushi, K. Nishihara, S. Okihara, T. Kagawa, Y. Izawa, K. Imasaki, T. Lida: Phys. Rev. A **69**, 023 203 (2004)
12 T. Ditmire, T. Donnelly, A.M. Rubenchik, R.W. Falcone, M.D. Perry: Phys. Rev. A **53**, 3379 (1996)
13 H.M. Milchberg, S.J. McNaught, E. Parra: Phys. Rev. E **64** 056 402 (2001)
14 C. Jungreuthmayer, M. Geissler, J. Zanghellini, T. Brabec: Phys. Rev. Lett. **92** 133 401 (2004)
15 P. Zhu, J. Liu, Z. Xu: Laser and Particle Beams **21**, 593 (2003)
16 J. Gspann: Electronic and Atomic Impacts on Large Clusters, *In Physics of Electronic and Atomic Collisions*, ed. by S. Datz (North Holland, Amsterdam 1982) p. 79
17 K.J. Mendham, N. Hay, M.B. Mason, J.W.G. Tisch, J.P. Marangos: Phys. Rev. A **64**, 055 201 (2001)
18 S. Zamith, Y. Ni, S.A. Aseyev, E. Springate, M.J. J Vrakking: Control of the production of highly charged ions in femtosecond laser cluster fragmentation, Femtochemistry and Femtobiology: Ultrafast Events in Molecular Science: VIth International Conference on Femtochemistry, Maison De La Chimie, Paris, France. July 6–10, 2003, **119**(4) (2003)
19 R. Trebino, K.W. Delong, D.N. Fittinghoff, J.N. Sweetser, M.A. Krumbugel, B.A. Richman, D.J. Kane: Rev. Sci. Inst. **68**, 3277 (1997)
20 G. Stobrawa, M. Hacker, T. Feurer, D. Zeidler, M. Motzkus, F. Reichel: Appl. Phys. B **72**, 627 (2001)
21 E. Zeek, A.P. Shreenath, P. O'Shea, M. Kimmel, R. Trebino: Appl. Phys. B **74** 265 (2002)
22 Y. Fukuda. K. Yamakawa, Y. Akahane, M. Aoyama, N. Inoue, H. Ueda, Y. Kishimoto: Phys. Rev. A **67**, 061 201 (2003)
23 T. Auguste, P.D'Oliveira, S. Huln, P. Monot, J. Abdullah, Jr, A.Y. Faenov, I.Y. Skobelev, A.I. Magunov, T.A. Pikuz: JETP Letters **72**, 38 (2000)
24 E. Springate, N. Hay, J.W.G. Tisch, M.B. Mason, T. Ditmire, J.P. Marangos, M.H.R. Hutchinson: Phys. Rev. A **61**, 044 101 (2000)
25 S. Zamith, T. Martchenko. Y. Ni, S.A. Aseyev, H.G. Muller, M.J.J. Vrakking: Phys. Rev. A **70**, 011 201 (2004)